Miniaturized HTS/Dielectric Multilayer Filters for Satellite Communications

Raymond S. Kwok* and S. Jerry Fiedziuszko
Space Systems/Loral, Palo Alto, CA 94303

Félix A. Miranda, Giadira V. Leon†, Melanie S. Demo‡, and Donna Y. Bohman
NASA Lewis Research Center, Cleveland, OH 44135

Abstract—**Presently, most communication satellites contain well over a hundred of filters in their payload. Typical satellite multiplexers use dual mode cavity or dielectric resonator filters which are large and heavy. As future advanced electronic systems for satellite communications become more complex, they will need even more filters requiring filter miniaturization without performance degradation. Therefore, any improvement in filter technology consistent with this requirement could enhance satellite's performance. To reduce the size, weight, and cost of the multiplexers without compromising performance, we introduce a new class of dual mode multilayer filters consisting of $YBa_2Cu_3O_{7-\delta}$ and $LaAlO_3$ thin films. The multilayer configuration in C-band, for example, occupies only 1% of the volume of its dielectric resonator counterpart. Details of the design, fabrication, and testing of these filters will be presented.**

I. INTRODUCTION

A major limiting factor in the continuing expansion of satellite communication systems is the lack of high performance (high Q) miniaturized filters which are compatible with microwave integrated circuits (MIC) and recently, monolithic microwave integrated circuits (MMIC) components. The major contribution to poor Q factor of the miniature, planar components is conductive loss, which can be significantly reduced by using superconducting materials. High Temperature Superconductivity has created a great deal of interest in replacing dual mode cavity and dielectric resonator filters with printed circuits which are dramatically smaller, lighter, and potentially less costly.

In this work, a new class of superminiature filters is described that is based on a multilayered stack of dual mode stripline or microstrip resonators coupled through irises. This filter configuration offers extremely small size and mass and can be fabricated using thin film superconductors. All filter types that are currently implemented using dual mode cavities or dielectric resonators can be realized using this novel filter structure. In this configuration, coupling between the dual mode resonators is controlled through irises similar to those used for the realization of cavity and dielectric resonator filters. The multilayer filter configuration has advantages over the previously introduced dual mode microstrip filters [1] in that it is smaller and lighter. This multilayer structure can be used to realize any of the filter types that are currently implemented using dual mode cavities or dielectric resonators including elliptic function and/or self-equalized responses. With continuing advances in superconductor fabrication this new class of filters is ideally suited for fabrication using High Temperature Superconducting (HTS) thin films for high Q performance. The HTS/dielectric Multilayer filters described in this work can be based on a variety of dual mode, planar resonator structures similar to those used in dual mode microstrip filters. These include square patches, circular disks, and rings [2]. Coupling between the dual orthogonal modes supported by these resonators is accomplished by introducing a perturbation to the symmetry of the previously single mode resonator at a location that is offset 45 degrees from the axes of coupling to and from the resonator.

II. EXPERIMENTAL

A. Filter Design

To show that the dual mode multilayer configuration can be implemented with HTS films and be integrated with a microstrip transmission line, a two-pole Chebyshev and a four-pole quasi-elliptical filters have been designed. A stripline dual mode square resonator is used to realize the two-pole filter response shown in Fig. 1. The next few paragraphs outline the calculation of the resonator's geometry.

For the corner-cut square resonator, the Mode Matching Method [3] cascaded with the Generalized Scattering Matrix [4] was proven to be effective. The 45 degree cut of a square resonator is first replaced by N number of equally-spaced steps as shown in Fig. 2. As N approaches infinity, the original geometry is recovered.

Within the cavity model, the electromagnetic field (for the lower half of the stripline) in the i^{th} region can be written as,

$$\vec{E}_i = \sum_n \cos(\beta_{in} x)\left[A_{in}^{-} e^{\gamma_{in} y} + A_{in}^{+} e^{-\gamma_{in} y}\right]\hat{z} \tag{1}$$

and

$$j\omega\mu\vec{H}_i = \hat{z} \times \nabla_t \vec{E}_i\ , \tag{2}$$

where γ_{in} is the complex propagation constant of the n^{th} mode in the i^{th} region, and ∇_t is the transverse component of the gradient operator. Note that the electromagnetic field in the upper half has the opposite sign.

Manuscript received August 27, 1996.

*Presently with Conductus, Inc., Sunnyvale, California.

†Permanent address: Department of Electrical Engineering, Rensselaer Polytechnic Institute, Troy, NY 12180.

‡Permanent address: Department of Electrical Engineering, Rice University, Houston, TX 77005.

1051-8223/97$10.00

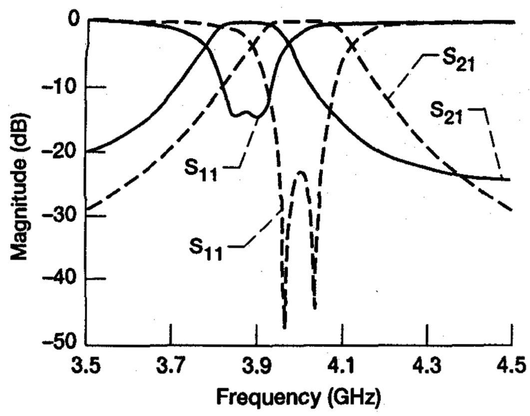

Fig. 1. Two-pole Chebyshev filter; prototype (dashed line) and Sonnet's em® simulator (continuous line).

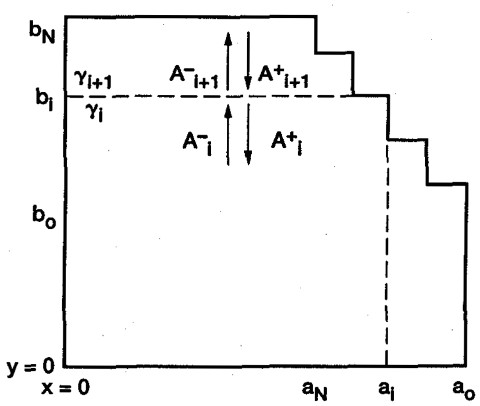

Fig. 2. Square resonator with corner-cut replaced by N number of equally-spaced steps.

The i^{th} discontinuity can be characterized by the S^i matrix defined by,

$$\begin{pmatrix} A_{i-1}^{-} \\ A_i^{+} \end{pmatrix} = \left(S^i\right) \begin{pmatrix} A_{i-1}^{+} \\ A_i^{-} \end{pmatrix}, \tag{3}$$

where (A_i^{+}) is a n-element column vector and (S^i) is a 2nx2n matrix. The (S^i) matrices are then combined with the adjacent step length (δ) through the transmission matrix (T^i) such that,

$$\left(\tilde{S}^i\right) = (T^i)\left(S^i\right)(T^i), \tag{4}$$

where,

$$(T^i) = \begin{pmatrix} I & 0 \\ 0 & \mathrm{diag}\left\{e^{-\gamma_i \delta}\right\} \end{pmatrix} \tag{5}$$

The process is shown pictorially in Fig. 3. These $\left(\tilde{S}^i\right)$ matrices are then cascaded together. Imposing the magnetic walls at the boundary of y=0 and y=b_N produced a singular

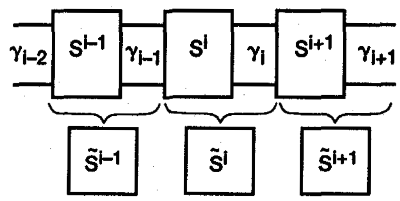

Fig. 3. Pictorial representation of the scattering matrix.

determinant from which the coupling coefficients are determined [2].

For the input and output couplings, a transmission line is tapped directly into the resonator at the two ports. The linewidth is modelled by a discontinuity capacitance [5]. With the calculated geometry, a computer simulation is produced using the Sonnet's em® simulator. These results are overlaid in Fig. 1.

The four-pole quasi-elliptical filter shown in Fig. 4 is designed by using the following coupling coefficients,

$$\left(M_{ij}\right) = \begin{pmatrix} 0 & 1.37 & 0 & -0.4 \\ 1.37 & 0 & 1.28 & 0 \\ 0 & 1.28 & 0 & 1.37 \\ -0.4 & 0 & 1.37 & 0 \end{pmatrix}. \tag{6}$$

Coupling between stripline layers is facilitated by a slot iris. The dimension is calculated using the small aperture approximation [6]. With no additional optimization, a proof-of-concept (POC) filter is built for each design. Measurements and results are presented in the following sections.

B. Filter Fabrication and Testing

The physical layout of a multilayer filter is shown in Fig. 5. The filter consists of two directly coupled, dual mode stripline resonators which are vertically stacked and coupled together through a cross iris in their common ground plane. Testing of this structure was performed by fabricating each of the layers of the stacked filter using gold (Au) and $YBa_2Cu_3O_{7-\delta}$ (YBCO) thin films on 508 μm thick single crystal lanthanum aluminate ($LaAlO_3$). Gold metallization

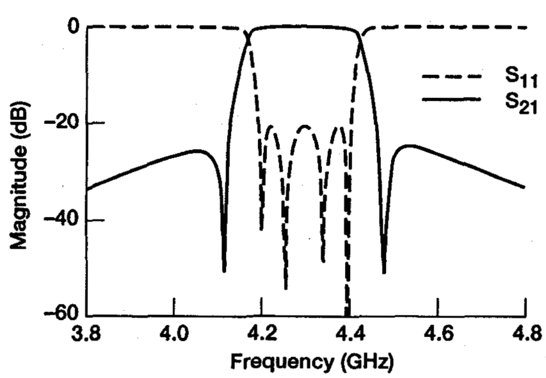

Fig. 4. Prototype response of a four-pole quasi-elliptical filter.

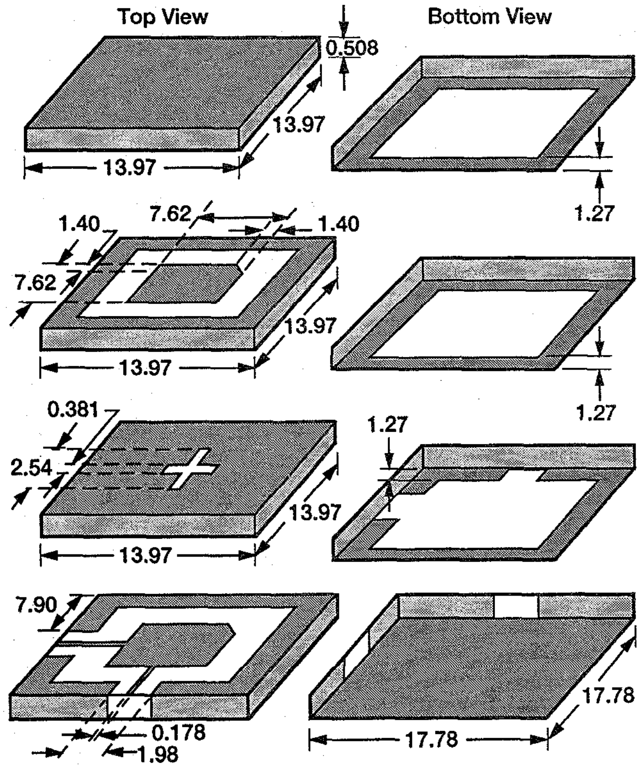

Fig. 5. Physical layout of a four-pole dual mode multilayer filter; dimensions are in mm.

was achieved by electron beam evaporation and consisted of 15 nm of chromium followed by a 2.5 μm thick gold layer. The gold circuit was defined using standard photolithography and chemical etching techniques. The HTS YBCO samples used in this study were obtained from a commercial vendor and had film thicknesses of approximately 350 nm. The circuit patterns of each of the layers of the structure were transferred to the YBCO films using standard photolithography techniques and wet etching (etch-back) with diluted phosphoric acid (H_2O:H_3PO_4 concentration of a 100:1). Typical transition temperatures of these films were 86 K as measured using a standard four-point-probe technique, indicating an uniform superconducting phase with appropriate oxygen stoichiometry [7].

The microwave characterization of these POC filters was performed at room temperature, for the Au version, and at cryogenic temperatures for the Au and YBCO versions. First, we tested the dual mode patch resonator in the microstrip configuration by mounting it on a brass test fixture custom made so as to allow for the coaxial-to-microstrip transition (accomplished through launchers with SMA connectors) and for attachment to the cold plate of a helium gas closed-cycle refrigerator. Fig. 6 shows the Au dual mode POC resonator mounted on the test fixture. To test the POC dual mode planar filter in the stripline and full multilayer stacked configuration, we mounted the layers shown in Fig. 5 on a brass test fixture featuring a top cross-bar bolted to the body of the fixture so as to allow tight contact between the layers comprising the filter. For the stripline configuration only the base dual mode patch

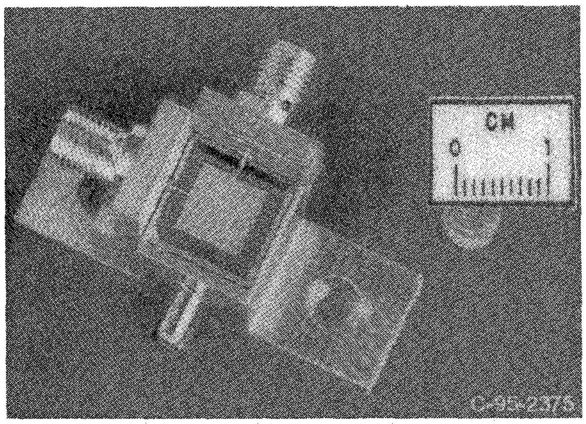

Fig. 6. Dual mode proof of concept (POC) gold resonator with corner-cut.

resonator and the second layer (without the coupling iris) were used. For the four-pole dual mode multilayer filter all the layers (with the coupling iris in the second layer) were used. Grounding of the structure was achieved by applying silver paint to the edges of the patch resonators' substrates. A picture of this configuration mounted inside the vacuum chamber of the closed-cycle refrigerator is shown in Fig. 7.

The reflection (S_{11}) and transmission (S_{21}) scattering parameters were measured using an HP-8510 C Network Analyzer. The coaxial semi-rigid test cables were calibrated up to the end of the fixture's launchers using standard Short-Open-Load-Thru (SOLT) calibration techniques. All the calibrations were performed at room temperature before the beginning of each measurement cycle. All measurements were performed under vacuum (pressure less than 1 mtorr).

III. Results

Fig. 1 shows the S_{11} and S_{21} data for the planar dual mode stripline resonator as modelled using Sonnet's em® software. Observe that the resonant frequency is very close to the design frequency of 4.0 GHz. Fig. 8 shows the measured performance of such a stripline resonator when implemented using Au (Fig. 8a) and single-sided YBCO thin film on $LaAlO_3$ (Fig. 8b). Note that both resonators perform at a

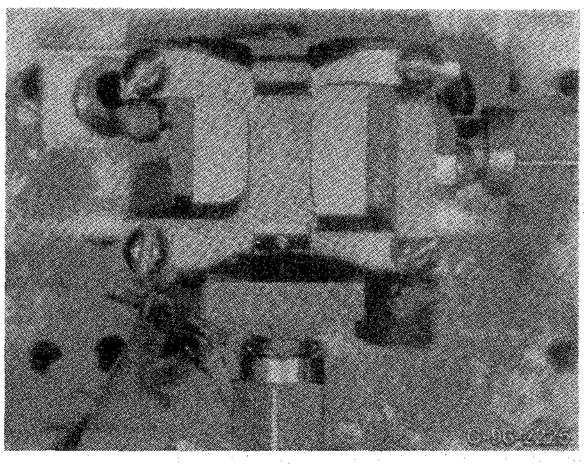

Fig. 7. Dual mode multilayer planar filter in test fixture for microwave measurements at cryogenic temperatures.

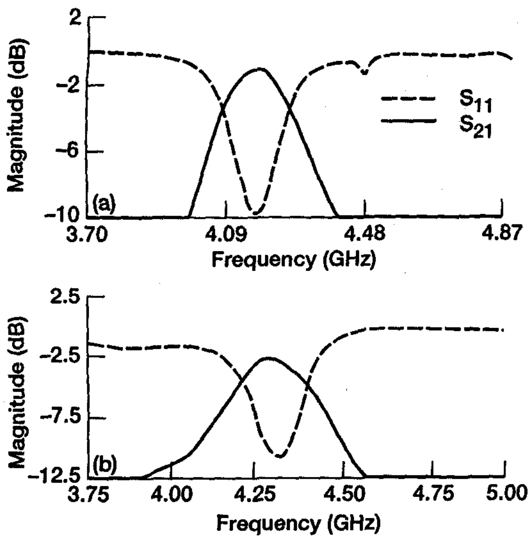

Fig. 8. Measured performance of stripline, 1.40 mm notch, one patch resonator at 77 K; (a) Au; (b) YBCO.

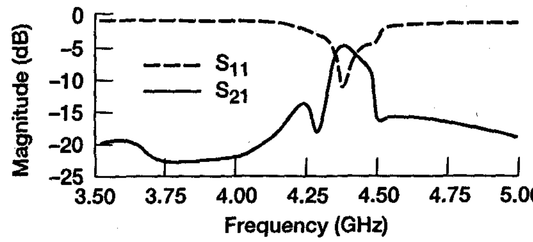

Fig. 9. Experimental performance of the full multilayer filter with a 7.11x7.11 mm patch, 0.508 mm notch, dual mode resonator as the first layer, and a 7.62x7.62 mm, 1.40 mm notch, dual mode resonator as the third layer.

frequency somewhat higher than that expected from the modelled data in Fig. 1. Also, the return (S_{11}) and insertion (S_{21}) losses of the Au version are superior to those of the YBCO resonator. This is contrary to what was expected from measurements of the resonators in the microstrip configuration where insertion losses of 0.96 dB for YBCO and of 2.52 dB for Au, and return losses of 11.13 dB for YBCO and of 7.98 dB for Au were obtained. We believe that this may be due to having more difficulties with optimizing the grounding between the YBCO layers (particularly contact between "window frames") as compared to that attained for the gold version of the resonator.

Fig. 9 shows the S_{11} and S_{21} data for the Au version of the POC dual mode multilayer filter as shown in Figs. 5 and 7. The performance shown was obtained by using a 7.11x7.11 mm patch, with a 508 μm notch, as the first layer dual mode resonator, and a 7.62x7.62 mm, 1.40 mm notch, dual mode resonator as the third layer of the multilayer filter. The corresponding notches were rotated 90 degrees with respect to each other to realize the negative coupling coefficient m_{14}. Clearly the coupling needs to be adjusted judging from the modelled data in Fig. 4. Nevertheless, the measurement reveals most of the design features including the finite transmission zeros by the passband. The upshifted measured frequency and suppression of some of the poles are expected due to loading effects of the input coupling line which were not fully accounted for in this work.

V. Conclusions

We have demonstrated the feasibility of fabricating multilayer HTS dual mode filters. The data presented in this work represent a proof-of-concept without tuning or optimi zation. To optimize the design, more work is required beyond the first approximation of our coupling structure calculations (i.e., a full wave analysis should be performed). The HTS/Dielectric Multilayer filters described in this work have great potential to solve the difficult problem of signal filtering in satellite and ground based communication systems. Simplicity of multilayer design and potential for mass production combined with high performance will ultimately result in low cost, which is crucial for wide application.

References

[1] J.A. Curtis and S.J. Fiedziuszko, "Miniature dual mode microstrip filters," *IEEE MTT-S Dig.*, pp. 443–446, June 1991.

[2] S.J. Fiedziuszko, J.A. Curtis, S.C. Holmes, and R.S. Kwok, "Low loss multiplexers with planar dual mode HTS resonators," *IEEE Trans. Microwave Theory Tech.*, vol. 44, pp. 1248–1257, July 1996.

[3] T. Itoh, "Numerical techniques for microwave and millimeter-wave passive structures," ed. T. Itoh, Ch. 9, Wiley & Sons, 1989.

[4] Y.C. Shih, "Numerical techniques for microwave and millimeter-wave passive structures," ed. T. Itoh, Ch. 10, Wiley & Sons, 1989.

[5] B. Bhat and S.K. Koul, "Stripline-transmission lines for microwave integrated circuits," Ch. 10, Wiley & Sons, 1989.

[6] G. Matthei, L. Young, and E.M.T. Jones, "Microwave Filters, Impedance-matching networks, and coupling structures," Ch. 5, Artech House, 1980.

[7] R.S. Kwok, S-W. Cheong, J.D. Thompson, Z. Fisk; J.L. Smith, J.O. Willis, "Perspective on RBa_2Cu_3Ox materials from oxygen deficiency studies," Physica C, vol. 152, p. 240–246 (1988).